Clays and Clay Minerals, 1969, Vol. 17, pp. 63–76. Pergamon Press. Printed in Great Britain

HYDRAULIC AND ELECTRICAL FLOWS IN CLAYS

KANDIAH ARULANANDAN
Department of Civil Engineering, University of California, Davis, California

(*Received* 14 *November* 1968)

Abstract—The electrical conductivity of saturated kaolinite clay–water–electrolyte systems of different particle size distributions and of illite and montmorillonite clays were determined over the frequency range of 50–10^8 c/s. The conductivity increases as the frequency increases, and the experimental values show two distinct dispersions, one in the low frequency range and the other in the high frequency range. The frequency range over which the first dispersion occurs is experimentally shown to be dependent on particle size. The average particle size is uniquely related to the frequency at which half the dispersion occurs. The magnitude of conductivity variation, the high frequency conductivity and the streaming potential values are related to the microscopic permeability coefficient. This microscopic permeability coefficient, evaluated from a knowledge of the above electrical properties, is shown to be uniquely related to the Darcy permeability coefficient at various consolidation states of the kaolinite clays. Similar unique relationships have been observed in illitic clays.

INTRODUCTION

THE EXPERIMENTALLY observed increase in electrical conductivity with an increase in alternating current frequency of a clay–water–electrolyte system (Fig. 1) is usually described as conductivity dispersion. This effect of frequency on conductivity has been observed for clays (Vacquier, *et al.* 1957; Olsen, 1959; Mitchell and Arulanandan, 1967), mineralized rocks (Madden and Marshall, 1959), polymers (Juda and McRae, 1953), synthetic membranes (Spiegler and Arulanandan, 1967, 1968), ion exchange resins (Sachs and Spiegler, 1964), and polystrene spheres (Schwan, 1966). The conductivity dispersion characteristics were either experimentally observed in the electrical frequency range 0–10^5 c/s or in the radio frequency range 10^6–10^8 c/s, but no experimental data on any of the above materials are reported over the entire frequency range from 0–10^8 c/s.

In the present work, the conductivity dispersion characteristics of kaolinite–clay–water–electrolyte systems of different particle sizes, and for illite and montmoronillonite clays are reported for a range of frequency from 50–10^8 c/s. The relationship between the nature of the conductivity dispersion in the low frequency range (characterized by the frequency at which half the dispersion occurs) and the average particle size of the clays is examined in the first part of the paper. The second part of the paper deals with the relationship between the microscopic permeability coefficient as evaluated from considerations of coupling between electro-osmotic water flow and current flow, and the Darcy permeability coefficient.

EXPERIMENTAL PROCEDURE

Electrical properties tests

Impedances in the low frequency range 50–10^5 c/s. were measured with a "Comparator" type 1605 AM (General Radio Corporation) and in the high frequency range with the "RX meter" (Boonton Radio Corporation, Division of Hewlett-Packard, Rockaway, New Jersey). Electrode polarization in the low frequency range and line impedance in the radio frequency range were eliminated by methods described earlier (Arulanandan, 1968; Sacks and Spiegler, 1964).

The measured impedances were interpreted in terms of a parallel capacitance and resistance network (Arulanandan, 1968), and the conductivity values at each frequency were obtained.

Consolidation-permeation streaming potential tests

Consolidation-permeation and streaming potential values were obtained on samples of clay after increments of consolidation pressures ranging from 0·05 to 6·4 kg/cm^2. The test cell is similar to the one used by Olsen (1959). Figure 2 shows a diagramatic sketch of the apparatus.

To insure complete saturation of the samples, they were placed in the test cell as slurries that were just sufficiently concentrated to prevent segregation of particle sizes. The loose material was gradually consolidated with seepage pressure and then with small load increments up to a consolidation pressure of 0·4 kg/cm^2, at which point the test cycle was begun by recording the first set of hydraulic and streaming potential data.

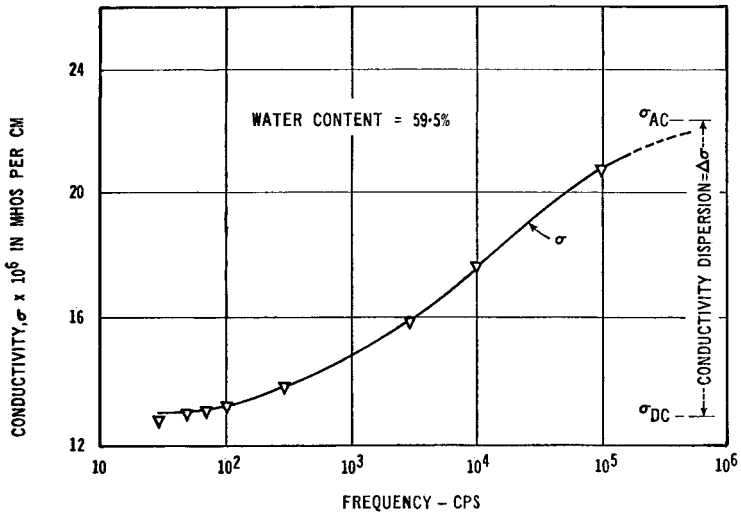

Fig. 1. Conductivity dispersion in kaolinite hydrite-R.

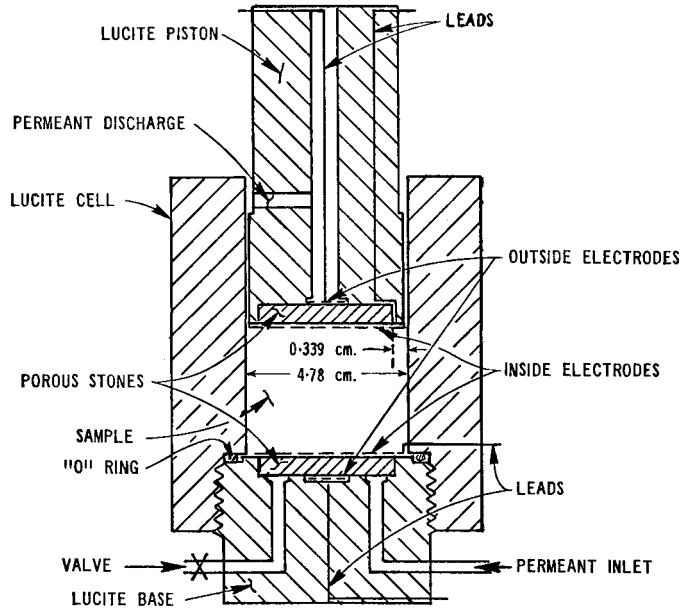

Fig. 2. Consolidation permeation test unit.

Upward permeation of a sample was produced by imposing a hydraulic gradient on the permeant (not exceeding 10 per cent of the consolidation pressure) by a vertical calibrated stand pipe that was attached to the base of the test cell. Flow rates were computed from the measured dimensions of the samples, the mean total flow rates, and the log mean hydrostatic heads.

For streaming potential measurements the cell was provided with electrodes at the bottom and top of the sample. The electrodes and leads were silver gauze and silver wire, coated electrolytically with silver chloride. Streaming potentials were measured with a Kiethley Electrometer attached to the electrodes. The slope of the streaming potential-hydraulic gradient relation was obtained from measurements of streaming potentials over a range of hydraulic permeation pressure gradients.

https://doi.org/10.1346/CCMN.1969.0170204 Published online by Cambridge University Press

Materials tested

The following systems were studied:

(1) Kaolinites (Hydrite MP, Hydrite 121, Hydrite R, Hydrite UF) which have different particle sizes and particle size distributions (Fig. 3) were made homo-ionic to Na, equilibrated with 0·001 N NaCl and consolidated from a slurry under 1·6 kg/cm^2 in all cases except in the case of Hydrite MP. The Hydrite MP was consolidated under 6·4 kg/cm^2 and allowed to rebound under 0·05 kg/cm^2. Conductivity dispersion characteristics were obtained over the range of frequency 50 c/s–10^8 c/s.

(2) Samples of illite Grundite and montmorillonite with particle sizes $< 2\,\mu$ were made homo-ionic to Na. Subsequently the samples were leached with distilled water and finally with approximately 0·001 N NaCl until the conductivity of effluent indicated that the soil water had these concentrations throughout. Samples were subjected to conductivity dispersion study.

(3) Kaolinite (Hydrite MP, Hydrite 121, Hydrite R, Hydrite UF) and illite (Grundite) clays were made homo-ionic to sodium chloride. The excess salt was then removed by leaching the clays with distilled water. The clays were subsequently dried in an oven at 230°F, lightly pulverized, and stored in sealed jars. Weighed amounts of each were later mixed with the desired electrolyte solution into thick slurries prior to their introduction into the appropriate cells for consolidation.

EXPERIMENTAL RESULTS

The results for clay–water–electrolyte systems are quite similar to those obtained for a biological cell suspension, Schwan (1957), and polystrene spheres (Schwan *et al.* 1966). The conductivity dispersion characteristics of the kaolinite water–electrolyte systems (item 1 above) as a function of particle sizes and particle size distributions are shown in Figs. 4 and 5. Similar results for illite and montmorillonite clays (item 2 above) are shown in Figs. 6 and 7.

It may be seen that there are two dispersions, one in the low and the other in the high frequency range. The frequency range over which the low frequency dispersion occurs is related to the particle size. The low frequency dispersion characteristics of kaolinite samples are plotted on an enlarged scale and shown in Fig. 8. The results are summarized in Table 1.

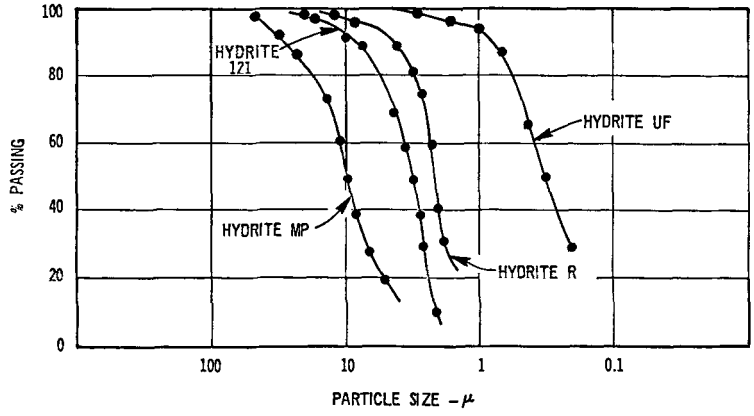

Fig. 3. Particle size distribution of different kaolinites.

Table 1

Clay type	Range of particle size (μ)	Range of low frequency dispersion (c/s)	Characteristic frequency (fo, c/s)
Hydrite MP	50–5	$1–3 \times 10^4$	150
Hydrite 121	20–2	$10–10^5$	3500
Hydrite R	10–1	$10–10^6$	40,000
Hydrite UF	5–0·5	$10–10^7$	300,000

https://doi.org/10.1346/CCMN.1969.0170204 Published online by Cambridge University Press

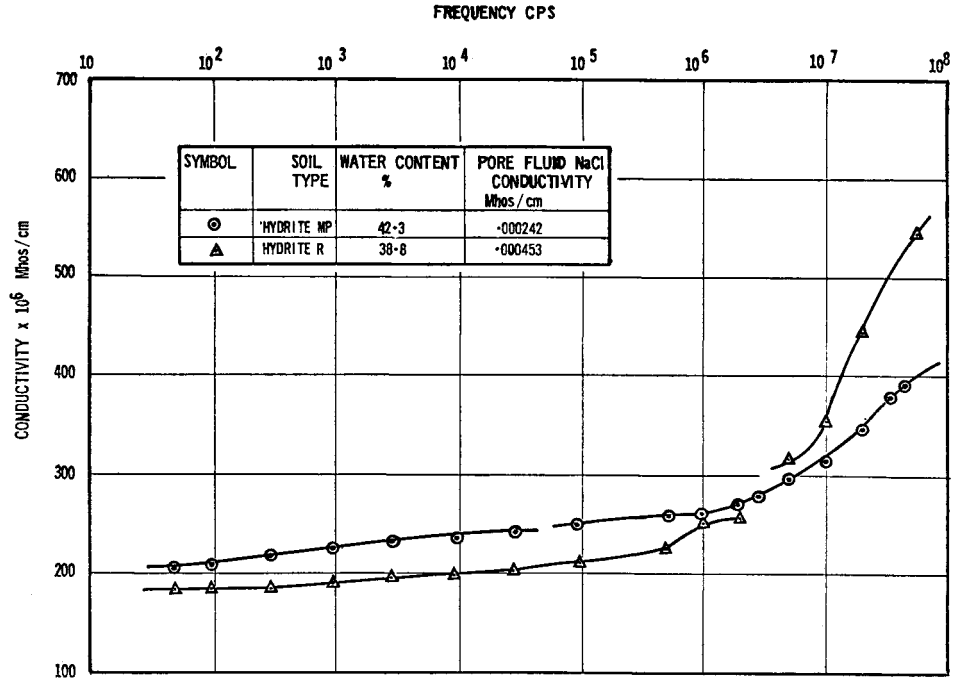

Fig. 4. Electrical and radio frequency range conductivity dispersion characteristics of sodium kaolinite samples consolidated from a slurry.

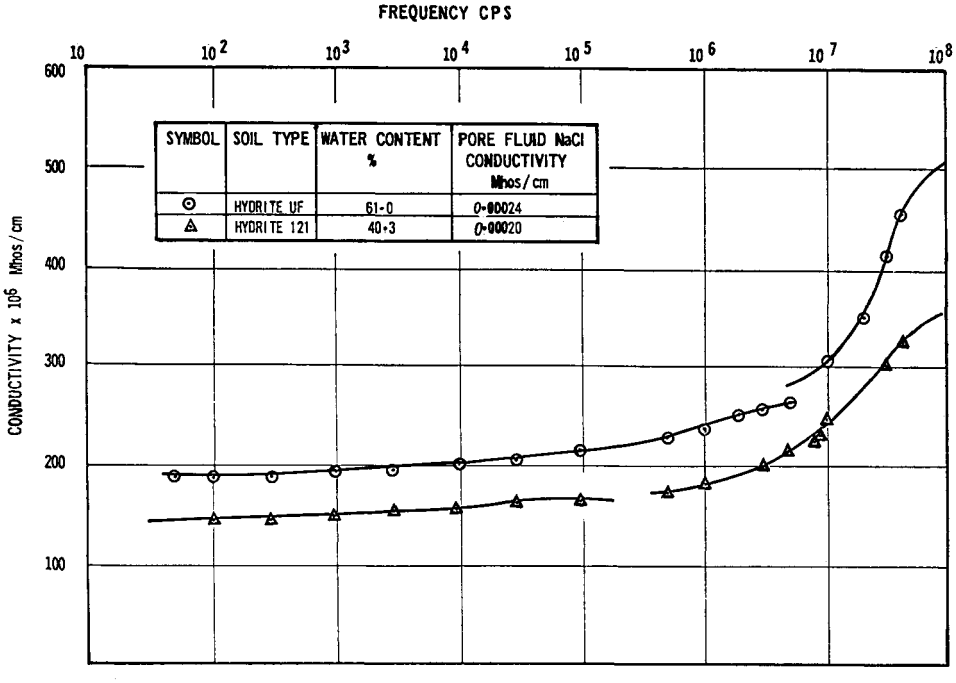

Fig. 5. Electrical and radio frequency range conductivity dispersion characteristics of sodium kaolinite samples consolidated from a slurry.

https://doi.org/10.1346/CCMN.1969.0170204 Published online by Cambridge University Press

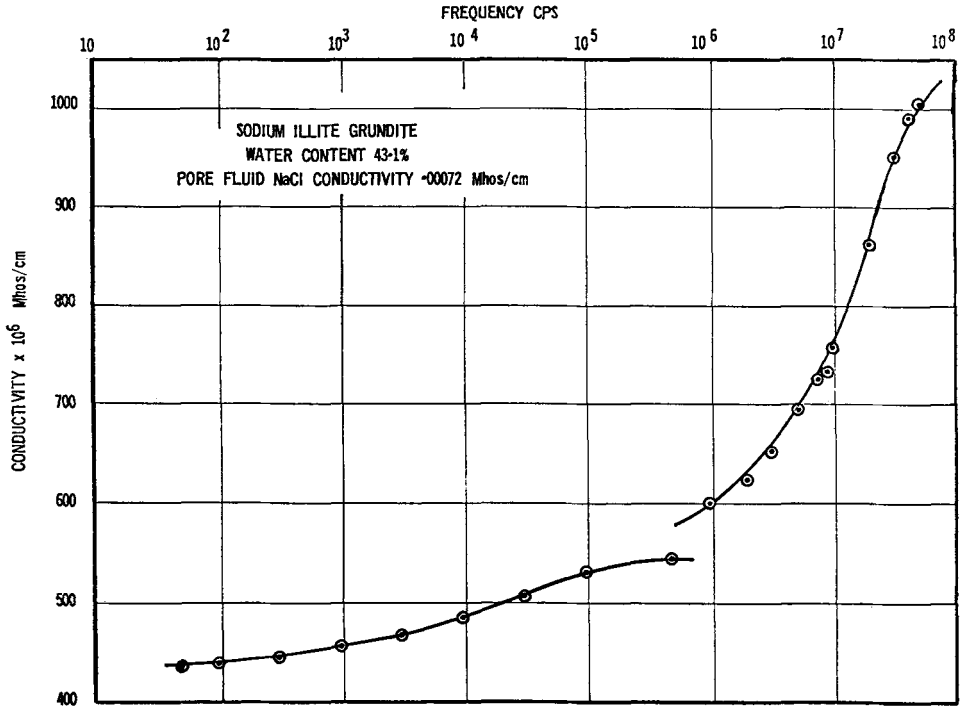

Fig. 6. Electrical and radio frequency range conductivity dispersion characteristics of sodium illite sample consolidated from a slurry.

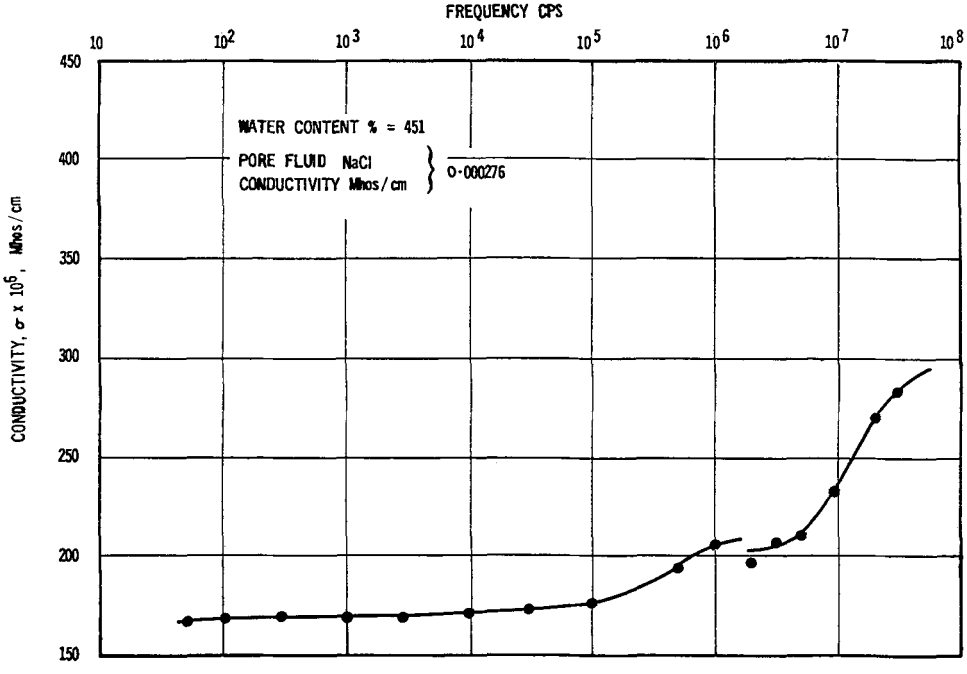

Fig. 7. Electrical and radio frequency range conductivity dispersion characteristics of sodium montmorillonite sample consolidated from a slurry.

https://doi.org/10.1346/CCMN.1969.0170204 Published online by Cambridge University Press

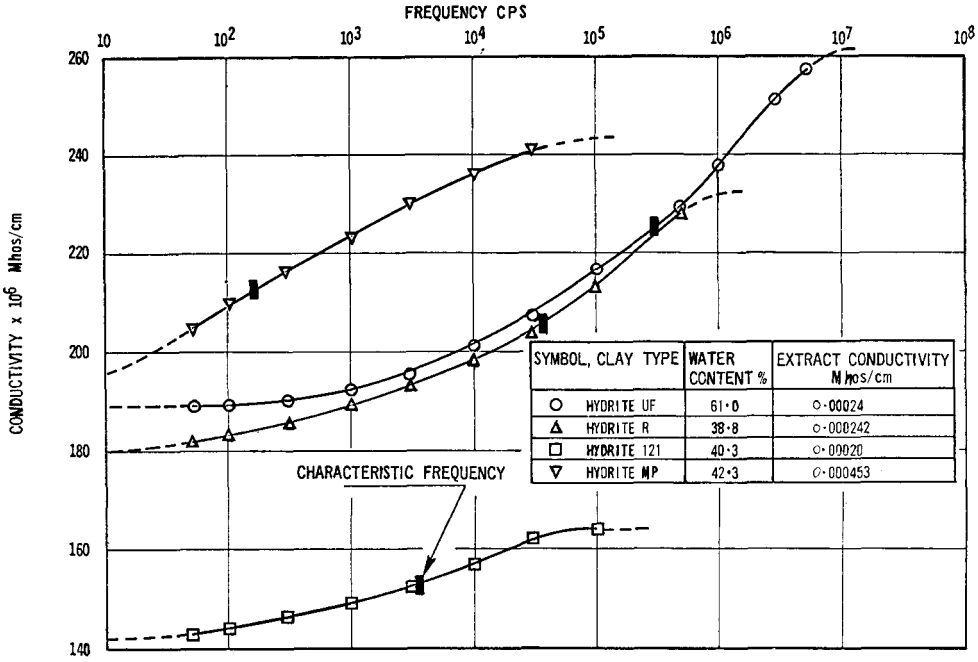

Fig. 8. Electrical frequency range conductivity dispersion characteristics of kaolinite samples consolidated from a slurry.

The larger the particle size, the lower is the range of frequency over which the dispersion occurs. The frequency at which half the conductivity dispersion occurs (which is referred to as the "characteristic" frequency) is smaller for the largest particle size sample.

The hydraulic permeability coefficients, streaming potential values and the conductivities σ_{DC} and σ_{AC} (see Fig. 1) obtained on a kaolinite and illite sample (item 3 above) when consolidated to different water contents are shown in Tables 2 and 3.

The hydraulic permeability and the streaming potential values are lower for the higher cation exchange capacity clay. The electrical permeability coefficients, derived by a theory to be described subsequently are shown at the bottom column of Tables 2 and 3, and are lower for the high cation exchange capacity clay and decrease with a decrease in water contents.

DISCUSSION

The results shown in Figs. 4, 5, 6 and 7 clearly indicate that there are two dispersions. Hence there should be two different mechanisms causing this frequency effect on conductivity. The mechanism causing the high frequency dispersion is to be discussed elsewhere ("Mechanism of Radio

Table 2. Consolidation permeation electrical dispersion and streaming potential results

Consolidation load (kg/cm²)	0·2	0·4	0·8	1·6	3·2	4·8	6·4	1·6	·05
Sample length, L (cm)	4·8274	4·7410	4·6280	4·4580	4·2165	4·0726	3·9327	3·9718	4·0600
Void ratio (e)	1·5105	1·4656	1·4068	1·3185	1·1930	1·1182	1·0454	1·0658	1·1180
Hydraulic conductivity ($k \times 10^6$ cm/sec)			11·90	9·16	6·86	4·69	4·02	4·57	5·38
Streaming potential (mv/atmos.)		57·00	56·10	50·40	47·40	37·90	35·20	41·40	43·20
$\sigma_{a.c.}$ in 10^{-4} Mhos/cm	3·04	3·01	2·98	2·84	2·65	2·66	3·16		
$\sigma_{d.c.}$ in 10^{-4} Mhos/cm	2·50	2·47	2·43	2·27	2·12	2·14	2·47		
Electrical permeability ($\times 10^7$ cm/sec)			5·08	3·59	2·98	1·95	1·79		

Clay: Kaolinite Hydrite MP; Permeant: 0·001 N NaCl; Temperature: 74°F.

https://doi.org/10.1346/CCMN.1969.0170204 Published online by Cambridge University Press

Table 3. Consolidation permeation electrical dispersion and streaming potential results

Consolidation load (kg/cm²)	0·4	0·8	1·6	3·2	4·8	6·4	1·6	0·5
Sample length, L (cm)	4·4373	4·0475	3·6876	3·3361	3·1554	3·0474	3·1071	3·3947
Void ratio (e)	1·7449	1·5039	1·2809	1·0629	0·9511	0·8843	0·9212	1·0988
Hydraulic conductivity ($k \times 10^8$ cm/sec)		5·011	4·390	2·511	1·520	0·860		
Streaming potential (mv/atmos.)	9·32	6·73	4·66	3·62	3·11	2·42		
$\sigma_{a.c.} \times 10^4$ Mhos/cm	4·60	4·43	7·10	7·20	6·85	7·30		
$\sigma_{d.c.} \times 10^4$ Mhos/cm	3·90	3·68	6·02	6·10	5·80	6·18		
Electrical permeability $\times 10^9$ cm/sec		1·152	0·982	0·599	0·419	0·270		

Clay: Illite; Permeant: 0·003 N NaCl; Temperature: 74°F.

Frequency Electrical Dispersion in Clays," Arulanandan and Spiegler, in preparation). The discussion here will be concerned with the mechanism of low frequency conductivity dispersion.

The existence of a frequency-independent, and consequently time-independent, tangential surface conductance has been proposed as being responsible for dispersion phenomena at low frequencies (C. T. O'Konski, 1960). It has been shown by Schwan (1962) that a frequency-independent purely-conductive surface layer, as considered by O'Konski, cannot explain the relaxation behavior. According to O'Konski's theory, the characteristic frequency should be in the upper Mc range, as has been shown by Schwan (1962).

It is considered by Schwan (1962), however, that the increase in conductivity with an increase in frequency in the low frequency range is due to the increase in surface conductance. The conductivity σ_0 of a clay–water electrolyte system can be expressed as

$$\sigma_0 = \sigma_a \frac{(1-p)}{1+p/2} + \frac{d}{R}\sigma_s \frac{4{\cdot}5p}{(1+p/2)^2}$$

where σ_a is the conductivity of the solution in equilibrium with the particles, p is the particle volume concentration, $d\sigma_s$ is the surface conductance, d is the thickness of the surface double layer, σ_s is the surface conductivity and R is the radius of the particles. The conductivity σ_0 consists of two parts, $\sigma_a\ (1-p)/1+p/2$ and $d/R\ \sigma_s\,(4{\cdot}5p)/(1+p/2)^2$. The first part is frequency independent at low frequencies. The term $d/R\ \sigma_s\,(4{\cdot}5p)/(1+p/2)^2$, however, is considered to be frequency dependent in the low frequency range. The value σ_s increases with increase in frequency and accounts for the conductivity dispersion. Such an analysis does not provide an insight into the physical mechanism causing its existence, but the frequency dependent component is a function of particle size, as seen from the data presented in Table 1.

The larger the particle size, the lower is the range of frequency over which the dispersion occurs, and the characteristic frequency is proportional to $1/R^2$, as seen from the results shown in Fig. 9. It can be shown (Moore, 1963, pp. 342–343) that the average distance traversed by diffusing ions is given by the mean square displacement $\overline{\Delta x^2}$. The average relaxation τ taken by the ions to traverse $\overline{\Delta x^2}$ and the diffusion coefficient D are related by the expression $\overline{\Delta x^2} = 2D$. This expression shows that $\tau \propto \overline{\Delta x^2}$. It is well known that $\tau = 1/2\pi f_0$, where f_0 is the characteristic frequency. Hence f_0 is inversely proportional to $1/\Delta x^2$. The results shown in Fig. 9 indicate that the characteristic frequency is inversely proportional as the square of the particle size. It is therefore reasonable to say that the process causing the electrical dispersion in the low frequency range is a diffusion controlled relaxation phenomena.

Magnitude of conductivity dispersion and electrokinetic phenomena

The application of an alternating current sets the ions in an oscillatory motion. In clays and other ion exchangers the positive counter-ions required to balance the negative fixed charges on the solid particles are in the majority, and hence they impart more momentum to the water than the co-ions. Thus there is a net water transfer in the direction of counter-ion movement. Use can be made of this principle to examine the relationship between the low frequency conductivity σ_{DC} and the high frequency conductivity σ_{AC} by considering the coupling between electro-osmotic water flow and current flow.

The relationship between steady state conductivities, microscopic permeability coefficient and streaming potential

Conventional flow processes and their coupling or interaction effects are schematically illustrated in Table 4. The best known and understood of these processes is that associated with coupling between solvent and electrical flows; i.e. electro-osmosis.

https://doi.org/10.1346/CCMN.1969.0170204 Published online by Cambridge University Press

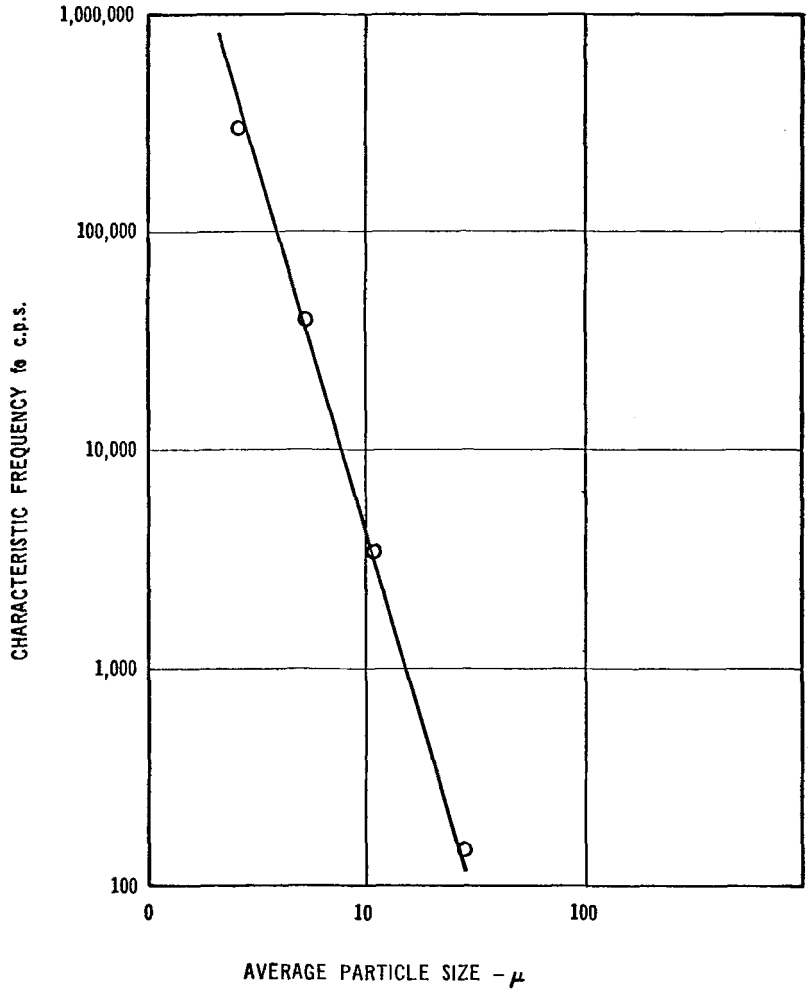

Fig. 9. Relationship between particle size and characteristic frequency.

Table 4. Coupled flow phenomena

Flow	Pressure gradient	Temperature gradient	Electric field	Chemical gradient
Fluid flow	Darcy's law hydraulic conductivity	Thermo-osmosis	Electro-osmosis	Normal osmosis
Heat flow	Isothermal heat transfer	Fourier's law heat conductivity	Peltier effect	Dufour effect
Current flow		Thermo-electricity	Ohm's law electric conductivity	Diffusion and membrane potentials
Ion flow	Streaming current	Soret effect thermal diffusion	Electro-phoresis	Fick's law diffusivity

https://doi.org/10.1346/CCMN.1969.0170204 Published online by Cambridge University Press

When a current is flowing in the system, there is a net water movement to accompany the current flow. When transport of liquid and electric charge occur simultaneously by electrical and hydrodynamic processes in membranes or porous media, they combine by simple addition in the following form (Lorenz, 1952, 1953).

$$J_v = L_{11}\,\Delta P + L_{12}\,\Delta E \tag{1}$$

$$I = L_{21}\,\Delta P + L_{22}\,\Delta E \tag{2}$$

where

J_v = Volume flux, cm³/sec
I = Current flux, amps
ΔP = Pressure drop across the diaphragm, dynes/cm²
ΔE = Electric potential across the diaphragm, volts
L_{ik} = Phenomenalogic transport coefficient.

We now define the d.c. and a.c. steady states in the following manner. If a low frequency current is passing through a system, there is enough time available for any pressure gradient to build up. Such a pressure gradient buildup will tend to oppose the flow of fluid. This pressure gradient will tend to oppose the volume flow. Thus in the d.c. steady state we have an electro-osmotic counter pressure which prevents the volume flow, i.e., $J_v = 0$.

From Eq. 1, for the condition $J_v = 0$

$$(\Delta P)_{e.o.c.p.} = -\frac{L_{12}}{L_{11}}\Delta E$$

where $e.o.c.p.$ = electro-osmotic counter pressure

$$\begin{aligned}(I)_{e.o.c.p.} &= L_{21}\,\Delta P + L_{22}\,\Delta E \\ &= L_{21}\left(-\frac{L_{12}}{L_{11}}\Delta E\right) + L_{22}\,\Delta E\end{aligned} \tag{3}$$

$$\sigma_{\text{d.c.}} = \sigma_{e.o.c.p.} = \frac{I_{e.o.c.p.}}{\Delta E} = -\frac{L_{21}L_{12}}{L_{11}} + L_{22}$$

where σ is the electrical conductivity.

At the high frequency, where the frequency of alternating current is large enough, a stage could be reached when sufficient time is not available for the buildup of a pressure gradient. This stage represents another condition under which the pressure gradient is zero, and there is no electro-osmotic counter pressure. Then from Eq. (2) one obtains

$$\sigma_{\text{a.c.}} = \left(\frac{I}{\Delta E}\right)_{\Delta P=0} = L_{22}. \tag{4}$$

From Eqs. (3) and (4),

$$\frac{\sigma_{\text{d.c.}}}{\sigma_{\text{a.c.}}} = 1 - \frac{L_{21}L_{12}}{L_{22}L_{11}}.$$

Also $(\Delta E/\Delta P)_{I=0} = \xi$ = streaming potential = $-(L_{21}/L_{22})$ from (2). Substituting $-(L_{21}/L_{22}) = \xi$ yields

$$\frac{\sigma_{\text{a.c.}}}{\sigma_{\text{d.c.}}} = \frac{1}{1 + \xi\dfrac{L_{12}}{L_{11}}}. \tag{5}$$

Using the condition

$$\left(\frac{J_v}{\Delta P}\right)_{I=0} \simeq \left(\frac{J_v}{\Delta P}\right)_{E=0} = L_{11} \quad \text{from (1).}$$

and Onsager's relationship $L_{21} = L_{12}$, we get from $\xi = -(L_{21}/L_{22})$.

$$L_{12} = -\xi\sigma_{\text{a.c.}}, \quad \text{since} \quad \sigma_{\text{a.c.}} = L_{22} \quad \text{from (4).}$$

Substituting for L_{12} the value of $-\xi_{\text{a.c.}}$ in (5) we get

$$\frac{\sigma_{\text{a.c.}}}{\sigma_{\text{d.c.}}} = \frac{1}{1 - \dfrac{\xi^2\sigma_{\text{a.c.}}}{L_{11}}} = \frac{1}{1 - \dfrac{\xi^2\sigma_{\text{a.c.}}}{k_m}}. \tag{6}$$

where k_m is the microscopic permeability coefficient electrically determined.

Property relationships

The main factors that affect permeability characteristics of saturated clays, when the permeant used is of the same type as that which exists in the soil, are the mineral composition, particle size distribution and particle orientation, void ratio, and exchangeable-cation composition. Electrical properties obtained as a function of frequency are also controlled by the above factors (Mitchell and Arulanandan, 1968). Hence, a relationship between the permeability coefficient obtained in terms of electrical properties K_m and the hydraulic permeability coefficient K_D, measured by conventional testing apparatus, may exist. To examine such a possibility, different samples of kaolinites and one sample of illite (item 3 under materials tested) were made homo-ionic to NaCl as close to 0·001 N as possible. Samples were consolidated to different water contents and at each water content the hydraulic permeability K_D and the electrical properties (ξ, $\sigma_{\text{d.c.}}$ and $\sigma_{\text{a.c.}}$)

https://doi.org/10.1346/CCMN.1969.0170204 Published online by Cambridge University Press

were measured. The value of K_m was calculated using Eq. 6, and the results obtained on kaolinite *MP* and illite samples are shown in Tables 2 and 3, and the relationship between K_D and K_m are shown in Figs. 10 and 11. Similar relationships obtained on kaolinite Hydrites UF, R and 121 are shown in Fig. 12. Experimental data of $\sigma_{d.c.}$, $\sigma_{a.c.}$, ξ and K_D have been obtained by Olsen (1960) on kaolinite and illite samples. These results have been used to calculate K_m, and the relationships between K_D and K_m shown in Figs. 13 and 14 are similar to those obtained in the present investigation.

Table 5 summarizes the relationship between clay particle sizes and the ratio K_D/K_m for the kaolinite clays. These results show that K_D/K_m is a function of particle size. The larger ratio of K_D/K_m is obtained for the clay containing the larger sizes.

Table 5

Soil Type	K_D/K_M	Electrolyte concentration
Hydrite MP	22	0·001 N
Hydrite 121	11·5	0·001 N
Hydrite R	8·5	0·001 N
Hydrite UF	5·0	0·001 N

CONCLUSIONS

The results of this investigation have revealed that clay–water–electrolyte systems display conductivity dispersions in the electrical and radio frequency ranges. The mechanism causing the dispersion is significantly affected by the particle size, and the process causing the dispersion is diffusion controlled. An estimate of the average particle size may well be made by measuring the electrical dispersion.

The microscopic permeability coefficient, evaluated from electrical properties ($\sigma_{d.c.}$, $\sigma_{a.c.}$, and ξ), has been shown to be uniquely related to Darcy permeability coefficient. This relationship appears to be controlled by particle sizes.

An expression relating K_D and K_m would enable the prediction of hydraulic permeability from a knowledge of the conductivity dispersion in the low frequency and the electro-osmotic flow. The conductivity dispersion characteristics would permit evaluation of $\sigma_{d.c.}$ and $\sigma_{a.c.}$ and the electro-osmotic flow. The conductivity dispersion characteristics would permit evaluation of $\sigma_{d.c.}$ and $\sigma_{a.c.}$ and the

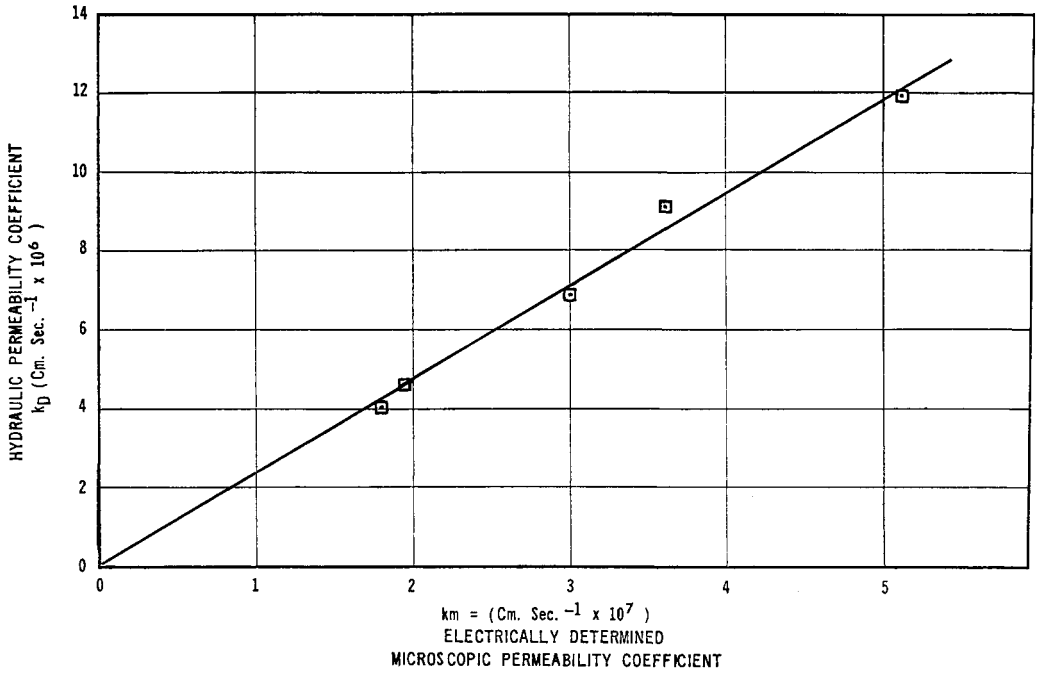

Fig. 10. Relationship between microscopic and hydraulic permeability coefficient during consolidation of a kaolinite-Hydrite MP made homoionic to 0·001 N NaCl.

https://doi.org/10.1346/CCMN.1969.0170204 Published online by Cambridge University Press

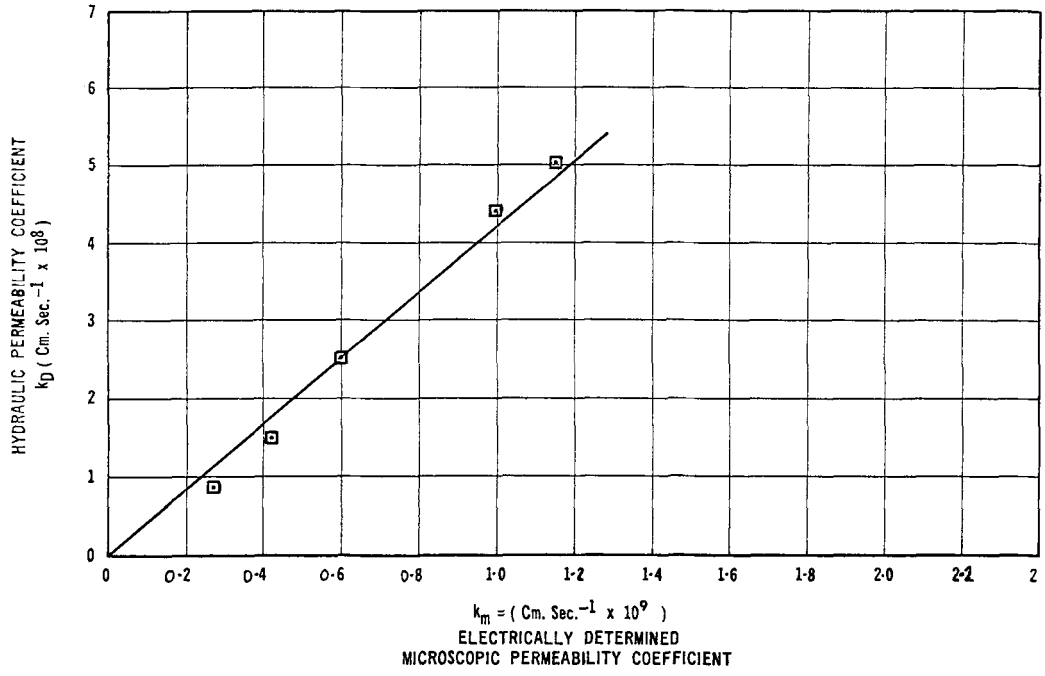

Fig. 11. Relationship between microscopic and hydraulic permeability coefficient during consolidation of an illitic clay < 2 μ made homoionic to 0·003 N NaCl.

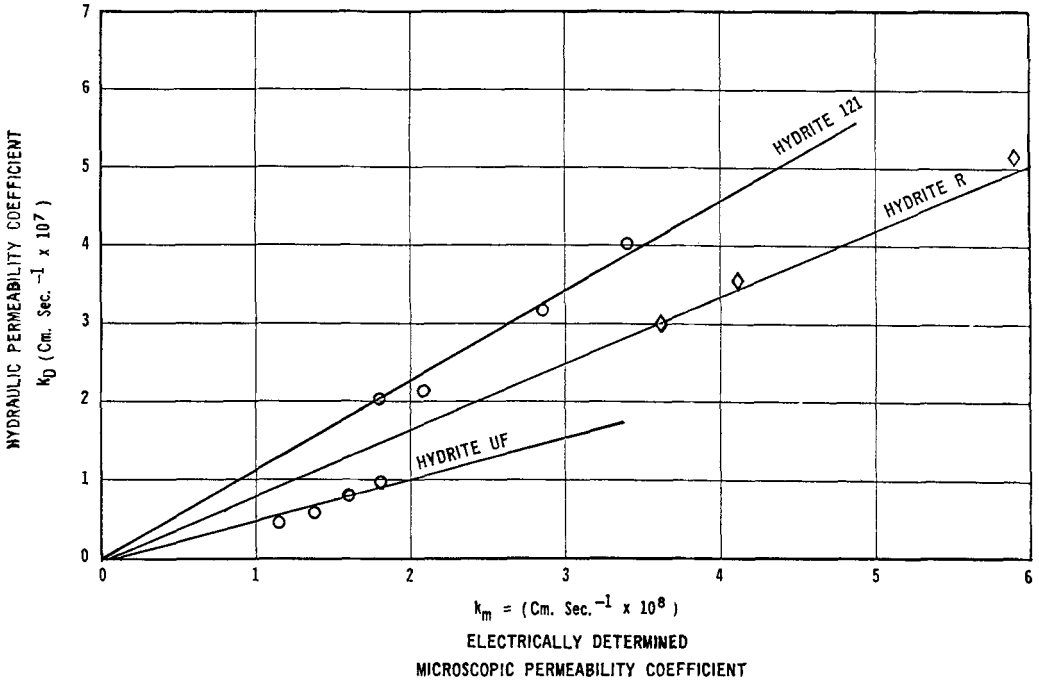

Fig. 12. Relationship between microscopic and hydraulic permeability coefficient during consolidation of kaolinite clays made homoionic to 0·001 N NaCl.

https://doi.org/10.1346/CCMN.1969.0170204 Published online by Cambridge University Press

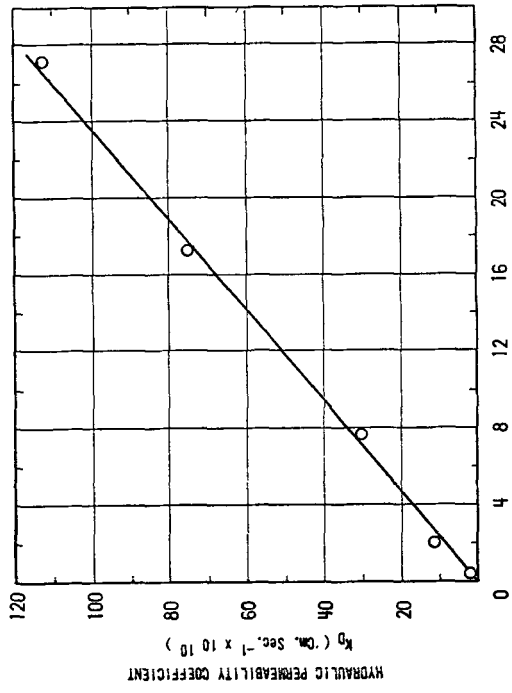

Fig. 14. Relationship between microscopic and hydraulic permeability coefficient during consolidation of an illitic clay $< 2\,\mu$ made homoionic to 0·001 N NaCl.

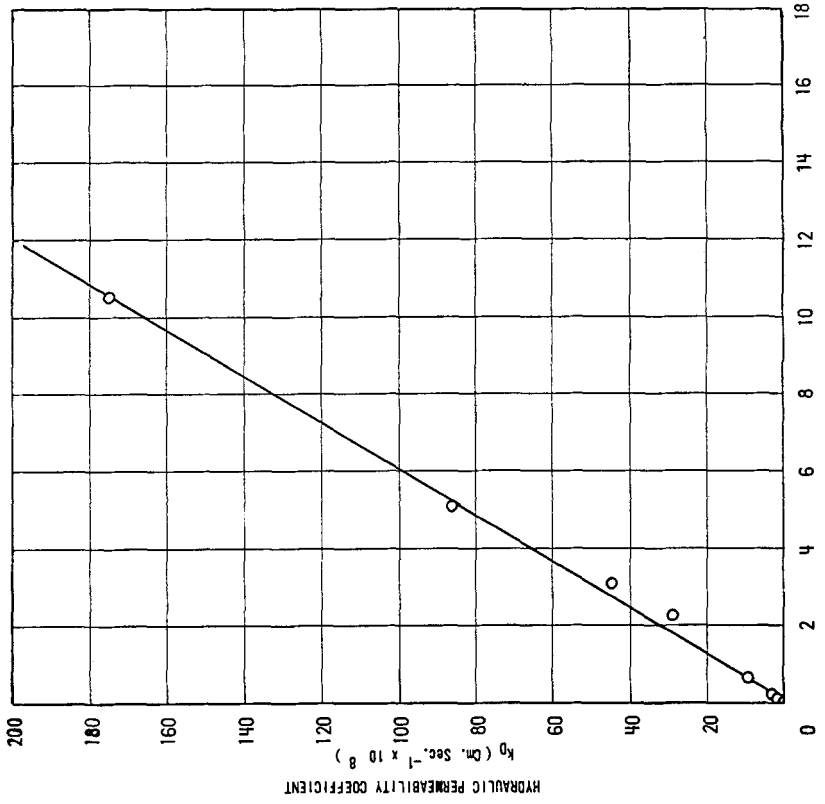

Fig. 13. Relationship between microscopic and hydraulic permeability coefficient during consolidation of a kaolinite clay of size $< 2\,\mu$ made homoionic to 0·0001 N NaCl.

https://doi.org/10.1346/CCMN.1969.0170204 Published online by Cambridge University Press

electro-osmotic flow data will enable the evaluation of ξ by the use of Saxen's Law which has been found to be applicable to clays (Gray, 1968). According to Saxen's Law, ξmV/atmos. $\times 54{\cdot}5 =$ Moles H_2O/Faraday.

Acknowledgments – The author wishes to thank Dr. K. S. Spiegler, Professor in Residence, University of California, Berkeley, for many interesting and valuable discussions concerning the subject of this paper.

The research comprised a part of an investigation of the relationship between electrical and mechanical properties of soils supported by National Science Foundation Grant No. GK-3539. The support is gratefully acknowledged.

REFERENCES

Arulanandan, K., and Mitchell, J. K. (1968) Low frequency dielectric disperions of clay–water–electrolyte systems: *Clays and Clay Minerals* **16**, 337–351.

Gray, D., and Mitchell, J. K. (1967) Fundamental aspects of electro-osmosis in soils: *J. Soil Mech. Found. Div. Am. Soc. Civil Engrs.* **93**, No. SM6, Proc. Paper 5580, 209–236.

Judy, W., and McRae, W. A. (1953) *U.S. pat.* 2,636,851.

Lorenz, P. B. (1952) The Phenomenology of Electro-Osmosis and Streaming Potential: *J. Phys. Chem.* **56**, 775–778.

Lorenz, P. B. (1953) Electro-kinetic relations in quartz-acetone systems: *J. Phys. Chem.* **57**, 430–434.

Madhen, T. R., and Marshall, D. J. (1958, 1959) Induced polarization study of the causes and magnitudes in geological materials: Final Reports for Atomic Energy Commission, Unpublished.

Mitchell, J. K., and Arulanandan, K. (1968) Electrical dispersion in relation to soil structure: *J. Soil. Mech. Found. Div.* SM2 5853.

Moore, Walter J. (1963) Physical Chemistry: 342–343.

O'Konski, C. T. (1960) Electric properties of macromolecules – V. Theory of ionic polarization polyelectrolytes: *J. Phys. Chem.* **64**, 605.

Olsen, H. W. (1959) Hydraulic Flow Through Saturated Clays: Thesis, M.I.T. Department of Soil Mechanics.

Sachs, S. B., and Spiegler, K. S. (1964) Radiofrequency measurements of porous conductive plugs, Ion-exchange resin-solution systems: *J. Phys. Chem.* **68**, 1214.

Schwan, H. P. (1957) Electrical properties of tissues and cell suspensions: *Biological and Medical Physics* **5**.

Schwan, H. P., *et al.* (1962) On the low frequency dielectric dispersion of colloidal particles in electrolyte solution: *J. Phys. Chem.* **66**, 2626.

Spiegler, K. S., and Arulanandan, K. (1968) Radiofrequency measurements of ion exchange membranes:

Spiegler, K. S., and Arulanandan, K. (1968) Radiofrequency measurements of ion exchange membranes: Research and Development report No. 353, U.S. Government Printing Office, Washington, D. C. Report to Office of Saline Water, U.S. Department of the Interior, Washington, D.C.

Vacquier, V., Holmes, C. R., Kintzinger, P. R., and Lavergne, M. (1957) Prospecting for ground water by induced electrical polarization: *Geophysics* **22**, 660–687.

Résumé – La conductivité électrique de systèmes saturés de kaolinite-eau-électrolyte à répartition variable des particles ainsi que d'argile du type illite en montmorillonite a été déterminée pour la gamme de fréquences allant de 50–10^8 périodes/sec. La conductivité augmente à mesure que la fréquence devient plus élevée et les valeurs expérimentales montrent deux dispersions distinctes, l'une dans la gamme de basses fréquences et l'autre dans la gamme de fréquences élevées. Les expériences montrent que la gamme de fréquences dans laquelle a lieu la première dispersion dépend des dimensions de la particule. La taille moyenne de la particule est en relation directe avec la fréquence à laquelle la moitié de la dispersion a lieu. L'importance de la variation de conductivité, la conductivité à fréquence élevée et les valeurs du potentiel d'écoulement sont mises en relation avec le coefficient de perméabilité microscopique. Le coefficient de perméabilité microscopique, évalué sur la base d'une connaissance des propriété électriques établies ci-dessus, est en relation directe avec la coefficient de perméabilité Darcy pour des états différents de consolidation des argiles du type kaolinite. Des relations du même genre ont été observées dans le cas des argiles illitiques.

Kurzreferat – Das elektrische Leitvermögen gesättigter Kaolinitton-Wasser-Elektrolytsysteme mit verschiedenen Teilchengrössenverteilungen und von Illit- und Montmorillonittonen wurde über einen Frequenzbereich von 50–10^8 Hz bestimmt. Das Leitvermögen wächst mit zunehmender Frequenz und die Versuchswerte zeigen zwei deutliche Streuungen, eine im Bereich der Niederfrequenzen und die andere im Bereich der Hochfrequenzen. Es wird durch Versuche dargelegt, dass der Frequenzbereich in welchem die erste Streuung auftritt von der Teilchengrösse abhängt. Die Durchschnittsgrösse der Teilchen steht in eindeutiger Beziehung zu der Frequenz bei welcher die Hälfte der Streuung auftritt. Der Schwinkungsbereich des Leitvermogens, das Hochfrequenzleitvermögen und die Strömungspotentialwerte stehen in Beziehung zum mikroskopischen Permeabilitätskoeffizienten. Es wird gezeigt, dass dieser aus der Kenntnis der obigen elektrischen Kenngrössen bestimmte mikroskopische Permeabilitätskoeffizient in den verschiedenen Verdichtungszuständen der Kaolinittone auf eindeutige Weise mit dem Darcy Permeabilitätskoeffizient in Verbindung steht. Ähnliche eindeutige Beziehungen sind auch bei den illitischen Tonen beobachtet worden.

Резюме—Удельная электропроводность систем насыщенная каолинитовая глина-вода-злектролит с распределением различных размеров частиц, а также иллитовых и монтмориллонитовых глин, определялась в диапазоне частот 50—10^8 *гц*. Электропроводность увеличивается по мере повышения частоты, а экспериментальные значения указывают две определенные дисперсии, одну в низкочастотном диапазоне, а вторуюбв-высокочастотном. Диапазон частот, в котором происходит первая дисперсия, зависит, как это доказано опытами, от размера частиц. Средний размер частиц уникально зависит от частоты, при которой происходит половина дисперсий. Величина изменений злектропроводности, высокочастотная проводимость и потенциалы течения зависят от коэффициента микроскопической проницаемости. Этот коэффициент микроскопической проницаемости, вычисленный на основании вышеуказанных электрических свойств, показан уникально зависящим от коэффициента проницаемости Дарси в различных стадиях консолидации каолинитовых глин. Сходная зависимость наблюдается и в иллитовых глинах.

https://doi.org/10.1346/CCMN.1969.0170204 Published online by Cambridge University Press